© 2018. Published by The Company of Biologists Ltd | Development (2018) 145, dev159970. doi:10.1242/dev.159970

RESEARCH ARTICLE

Ldb1- and Rnf12-dependent regulation of Lhx2 controls the relative balance between neurogenesis and gliogenesis in the retina

Jimmy de Melo[1], Brian S. Clark[1], Anand Venkataraman[1], Fion Shiau[1], Cristina Zibetti[1] and Seth Blackshaw[1,2,3,4,5,‡]

ABSTRACT

Precise control of the relative ratio of retinal neurons and glia generated during development is essential for visual function. We show that *Lhx2*, which encodes a LIM-homeodomain transcription factor essential for specification and differentiation of retinal Müller glia, also plays a crucial role in the development of retinal neurons. Overexpression of *Lhx2* with its transcriptional co-activator *Ldb1* triggers cell cycle exit and inhibits both Notch signaling and retinal gliogenesis. *Lhx2*/*Ldb1* overexpression also induces the formation of wide-field amacrine cells (wfACs). In contrast, *Rnf12*, which encodes a negative regulator of LDB1, is necessary for the initiation of retinal gliogenesis. We also show that Lhx2-dependent neurogenesis and wfAC formation requires *Ascl1* and *Neurog2*, and that Lhx2 is necessary for their expression, although overexpression of *Lhx2*/*Ldb1* does not elevate expression of these proneural bHLH factors. Finally, we demonstrate that the relative level of the LHX2-LDB1 complex in the retina decreases in tandem with the onset of gliogenesis. These findings show that control of *Lhx2* function by *Ldb1* and *Rnf12* underpins the coordinated differentiation of neurons and Müller glia in postnatal retina.

KEY WORDS: Cell fate, Co-factor, Gliogenesis, Neurogenesis, Retina, Transcription factor

INTRODUCTION

Lhx2 is one of 12 genes that make up the LIM class homeodomain (LIM-HD) family of transcription factors (TFs). *Lhx2* is dynamically expressed in multiple tissues, including discrete domains within the central nervous system (CNS) (Porter et al., 1997; Monuki et al., 2001). In the developing visual system, *Lhx2* activation is concurrent with patterning of the optic primordia and remains ubiquitous during formation of the optic vesicle and optic cup (Porter et al., 1997; Zuber et al., 2003). *Lhx2* is expressed in retinal progenitor cells (RPCs) throughout retinogenesis, ultimately becoming restricted to Müller glia (MG) and to a subset of amacrine interneurons (de Melo et al., 2012; Balasubramanian et al., 2014).

Germline deletion of *Lhx2* results in complete anophthalmia (Porter et al., 1997). However, conditional neuroretinal knockout of *Lhx2* (*Lhx2*ΔcKO) during later retinogenic timepoints results in premature cell cycle exit, altered RPC competence, loss of neuroretinal-derived FGFs (which results in a secondary arrest in lens fiber development) and disrupted MG development (Gordon et al., 2013; de Melo et al., 2016a; Gueta et al., 2016; Thein et al., 2016). The differentiation of neurons generated following *Lhx2*ΔcKO-induced cell cycle exit appears grossly normal, although neuronal diversity is limited by RPC competence at the stage when mitotic exit occurs (Gordon et al., 2013). *Lhx2* functions similarly in progenitor cells in the cerebral cortex, where it is essential for maintaining proliferative competence and developmental multipotency (Chou and O'Leary, 2013).

Lhx2 is essential for multiple aspects of retinal gliogenesis, with early *Lhx2* loss of function resulting in RPC dropout prior to the onset of gliogenesis. *Lhx2*ΔcKO at later timepoints yields disrupted Müller differentiation, leading to morphological abnormalities and a loss of MG-specific gene expression (de Melo et al., 2016a,b). *Lhx2*ΔcKO in fully differentiated mature MG causes cell-autonomous initiation of hypertrophic Müller gliosis in the absence of injury (de Melo et al., 2012). The effect of *Lhx2*ΔcKO on both RPC maintenance and gliogenesis may be mediated in part by *Lhx2*-dependent activation of genes in the Notch signaling pathway. *Lhx2* is a direct transcriptional regulator of multiple Notch pathway genes in both the retina (de Melo et al., 2016a) and cerebral cortex (Chou and O'Leary, 2013). Notch signaling regulates the maintenance of multipotent RPCs through the downstream activation of the Hes family members *Hes1* and *Hes5*, before ultimately promoting gliogenesis through the repression of proneural bHLH genes (Artavanis-Tsakonas et al., 1999; Mizeracka et al., 2013; Huang et al., 2014).

The molecular mechanisms that control the pleiotropic and context-dependent functions of *Lhx2* are unclear. However, several different transcriptional co-factors function as either co-activators or co-repressors with LHX2 proteins. LIM-HD transcriptional activator function is dependent on the formation of protein complexes with LIM domain-binding (LDB) co-factors (Matthews et al., 2008). Targeted loss of function of *Ldb* genes phenocopies targeted disruption of LIM-HD genes (Becker et al., 2002). Knocking out *Ldb1* with *Ldb2* in RPCs phenocopies *Lhx2*ΔcKO (Gueta et al., 2016), as does misexpression of a dominant-negative (DN) form of *Ldb1* in hippocampal progenitors (Subramanian et al., 2011). Expression of *Rnf12* (also known as *Rlim*), which encodes a RING finger LIM domain-interacting nuclear ubiquitin ligase, has been shown to result in the degradation of LDB proteins complexed with LIM-HD TFs, and thereby negatively regulates the transcriptional activity of LIM-HD TFs (Ostendorff et al., 2002; Hiratani et al., 2003). However, *Rnf12* has not been studied in the context of neuronal development.

[1]Solomon H. Snyder Department of Neuroscience, Johns Hopkins University School of Medicine, Baltimore, MD 21205, USA. [2]Department of Ophthalmology, Johns Hopkins University School of Medicine, Baltimore, MD 21205, USA. [3]Department of Neurology, Johns Hopkins University School of Medicine, Baltimore, MD 21205, USA. [4]Center for Human Systems Biology, Johns Hopkins University School of Medicine, Baltimore, MD 21205, USA. [5]Institute for Cell Engineering, Johns Hopkins University School of Medicine, Baltimore, MD 21205, USA.

‡Author for correspondence (sblack@jhmi.edu)

J.d.M., 0000-0001-9393-9217; A.V., 0000-0001-6303-4820; C.Z., 0000-0003-4922-1245; S.B., 0000-0002-1338-8476

Received 29 September 2017; Accepted 29 March 2018

Development (2018) 145, dev159970. doi:10.1242/dev.159970

In this study, we have investigated the role played by *Lhx2*-interacting transcriptional co-regulators during mammalian postnatal retinal development. We find that misexpression of *Lhx2*, in combination with *Ldb1*, in the neonatal mouse retina results in increased development of rod photoreceptors at the expense of MG and bipolar interneurons. Misexpression of *Lhx2* also drives a dramatic shift in amacrine cell (AC) morphology from narrow-field diffuse patterns to wide-field stratified patterns. We show that *Lhx2* directly regulates expression of multiple bHLH factors, and that the effects observed following misexpression are dependent on *Ascl1* and *Neurog2*. In contrast, we show that co-expression of *Rnf12* with *Lhx2* is both necessary and sufficient for Müller gliogenesis. These results identify a unique molecular switching mechanism that regulates the balance of retinal neurogenesis and gliogenesis through direct interaction with *Lhx2*.

RESULTS

Overexpression of *Lhx2* blocks Müller gliogenesis, and drives formation of rod photoreceptors and wide-field amacrine cells (wfACs)

To examine the effect of misexpression of *Lhx2* on retinal development, we electroporated postnatal day (P)0 mice with control (pCAGIG) and *Lhx2*-expressing (pCAGIG-Lhx2) DNA constructs (Fig. 1A-J). *Lhx2* electroporation promoted the generation of rod photoreceptors at the expense of both MG and bipolar interneurons (Fig. 1C,D). Fewer than 1% of *Lhx2*-electroporated cells expressed either of the two MG markers $P27^{Kip1}$ or GLUL, compared with nearly 5% of controls (Fig. 1D), and there was a significant reduction in cells with radial morphology (Fig. 1B,H-J). We also observed altered morphology among electroporated ACs (Fig. 1A,B arrows; Fig. S1A-C). Narrow-field, diffusely arborizing ACs were generated in control electroporations (Fig. 1A), whereas *Lhx2*-electroporated RPCs generated wfACs with distinct inner plexiform layer stratification into sublamina s1, s3 and s5 (Fig. 1B; Fig. S1A, arrow). Co-labeling of generated wfACs with AC subtype markers revealed that these cells did not express markers associated with any distinct AC subtypes, and only co-labeled with the pan-AC marker PAX6 (Fig. S1D-M arrows; Fig. S5; retina in Fig. S1D is also imaged at lower magnification in Fig. S5B).

Overexpression of *Lhx2* promotes cell cycle exit and downregulation of Notch signaling

Because *Lhx2* electroporation resulted in a loss of MG and bipolar interneurons, both populations being among the last cell types generated in the retina, we tested whether *Lhx2* overexpression

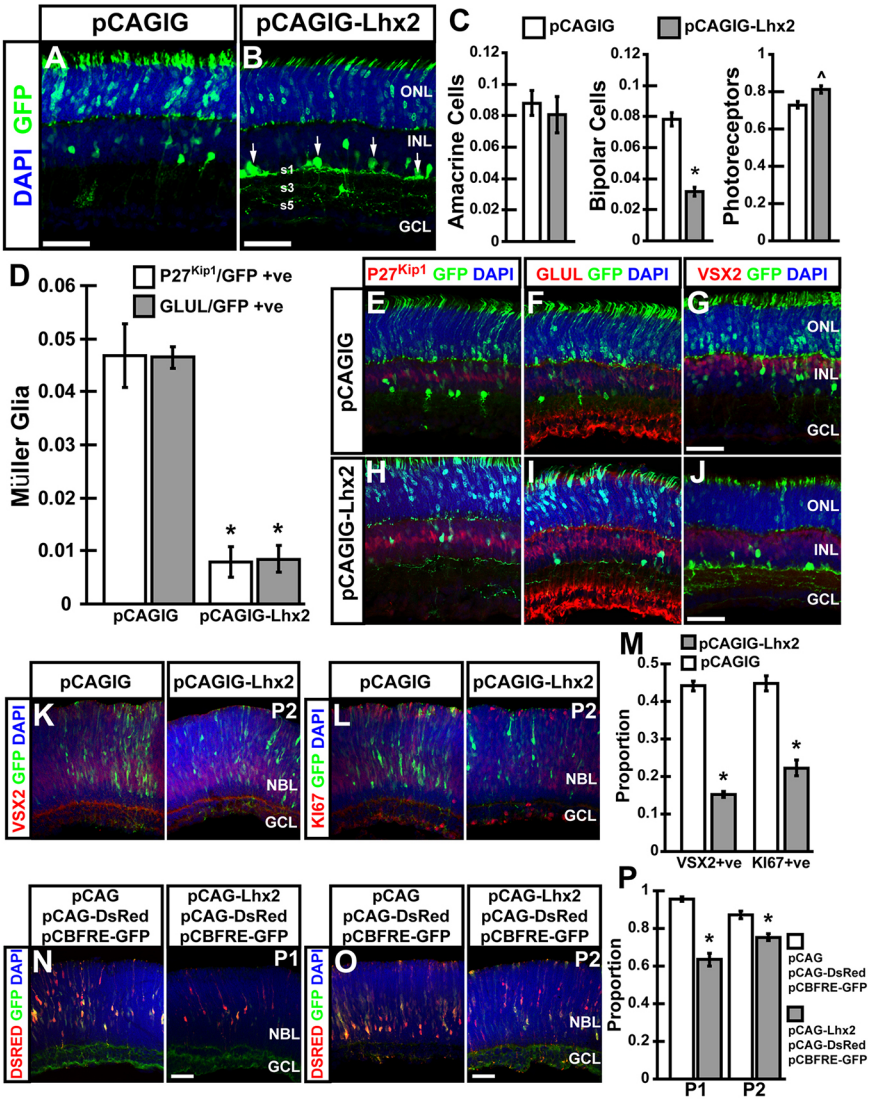

Fig. 1. Electroporation of *Lhx2* blocks Müller gliogenesis, bipolar cell formation and changes amacrine cell morphology.
(A,B,D-F,H,I) Electroporation of *Lhx2* resulted in a significant (P<0.05) decrease in Müller glia at P14 ($P27^{Kip1+}$ and $GLUL^{+}$) (4.68±0.60%, n=6, $P27^{Kip1}$ and 4.65±0.21%, n=6 GLUL versus 0.8±0.29%, n=6, $P27^{Kip1}$ and 0.85±0.25%, n=6, GLUL). (A-C,G,J) *Lhx2* electroporation resulted in decreased (P<0.05) numbers of bipolar interneurons ($VSX2^{+}$) (7.81±0.38%, n=6 versus 3.17±0.26%, n=6) and increased photoreceptors (77.3±2.4%, n=5 versus 82.44±2.1%, n=5). (B) Amacrine cell morphology changed from narrow field cells with diffuse dendrites to wide-field amacrine cells, which stratified into the S1, S2 and S3 sublamina of the inner plexiform layer (white arrows). (K-M) Cells electroporated with pCAGIG-Lhx2 at P0 showed significant (P<0.05) downregulation of both VSX2 and KI67 by P2. pCAGIG: 45.75±2.6%, n=5, VSX2; 44.8±1.79%, n=5, KI67. pCAGIG-Lhx2: 15.3±0.42%, n=5, VSX2; 22.8±1.97%, n=5, KI67. (N-P) Electroporation of *Lhx2* at P0 results in a significant decrease (P<0.05) of pCBFRE-GFP Notch reporter expression at P1 and P2. pCAG: 95.49±0.4%, n=5, P1; 87.34±1.57%, n=5, P2. pCAG-Lhx2: 63.43±2.86%, n=5, P1; 75.39±1.5%, n=5, P2. *Statistically significant decrease. ^Statistically significant increase. GCL, ganglion cell layer; INL, inner nuclear layer; NBL, neuroblastic layer; ONL, outer nuclear layer; P, postnatal day; s, inner plexiform layer sublamina. Data are mean±s.e.m. Scale bars: 50 µm.

Development (2018) 145, dev159970. doi:10.1242/dev.159970

affected the timing of RPC cell cycle exit (Fig. 1K-M). Electroporation of *Lhx2* resulted in premature cell cycle dropout and progenitor depletion by P2 (Fig. 1M). The number of cells co-labeled with the RPC marker VSX2 was reduced from 44% in controls to 15% in cells overexpressing *Lhx2* (Fig. 1M). Similarly, the number of electroporated cells co-labeled with the proliferation marker KI67 was reduced from 45% in controls to 22% with *Lhx2* (Fig. 1M).

As *Lhx2* electroporation promoted rod photoreceptor production at the expense of bipolar cells and MG, a process that requires the inhibition of Notch signaling in newly post-mitotic retinal precursors (Mizeracka et al., 2013), we tested whether Notch signaling was suppressed in *Lhx2* electroporated cells. P0 retinas were co-electroporated with a pCAG-DsRed cell reporter, pCBFRE-GFP Notch signaling reporter, and either pCAG control or pCAG-Lhx2 construct (Fig. 1N-P). Analysis at P1 and P2 revealed significant decreases in Notch reporter labeling in cells electroporated with *Lhx2* compared with controls (95% versus 63% at P1, $P<0.05$, $n=5$; 87% versus 75% at P2, $P<0.05$, $n=5$) (Fig. 1P). Taken together, these results show that electroporation of *Lhx2* results in rapid cell cycle dropout and downregulation of Notch signaling.

Lhx2 regulates neurogenesis and neuronal differentiation in part by regulation of proneural bHLH gene expression

The phenotype resulting from misexpression of *Lhx2* closely mirrors that of *Lhx2* loss of function (de Melo et al., 2016a). To determine why *Lhx2* misexpression might phenocopy *Lhx2* loss of function, we first analyzed the expression of multiple proneural bHLH genes, as well as *Hes6*, in an *Lhx2* ΔcKO model using the *Pdgfrα-Cre; Lhx2$^{lox/lox}$* mouse line. In these animals *Lhx2* is deleted from late-stage RPCs, resulting in a loss of MG and consequent photoreceptor degeneration (de Melo et al., 2016a) (Fig. S2). RNA-seq data obtained from *Pdgfrα-Cre; Lhx2$^{lox/lox}$* mice (de Melo et al., 2016a), showed substantially reduced expression, relative to controls, of multiple bHLH genes, including *Neurod1*, *Neurod4*, *Neurog2*, *Ascl1*, *Hes6* and *Olig2* (Table S1). We performed *in situ* hybridization to validate these results, and found that expression of each of these genes was reduced in *Pdgfrα-Cre; Lhx2$^{lox/lox}$* mice (Fig. 2A-F; arrows). These data suggest that *Lhx2* is necessary not only for expression of gliogenic bHLH factors in RPCs, as described previously (de Melo et al., 2016a), but also for multiple proneural bHLH factors. We tested whether Lhx2 might directly regulate expression of these genes by conducting ChIP-qPCR, examining evolutionarily conserved candidate *cis*-regulatory

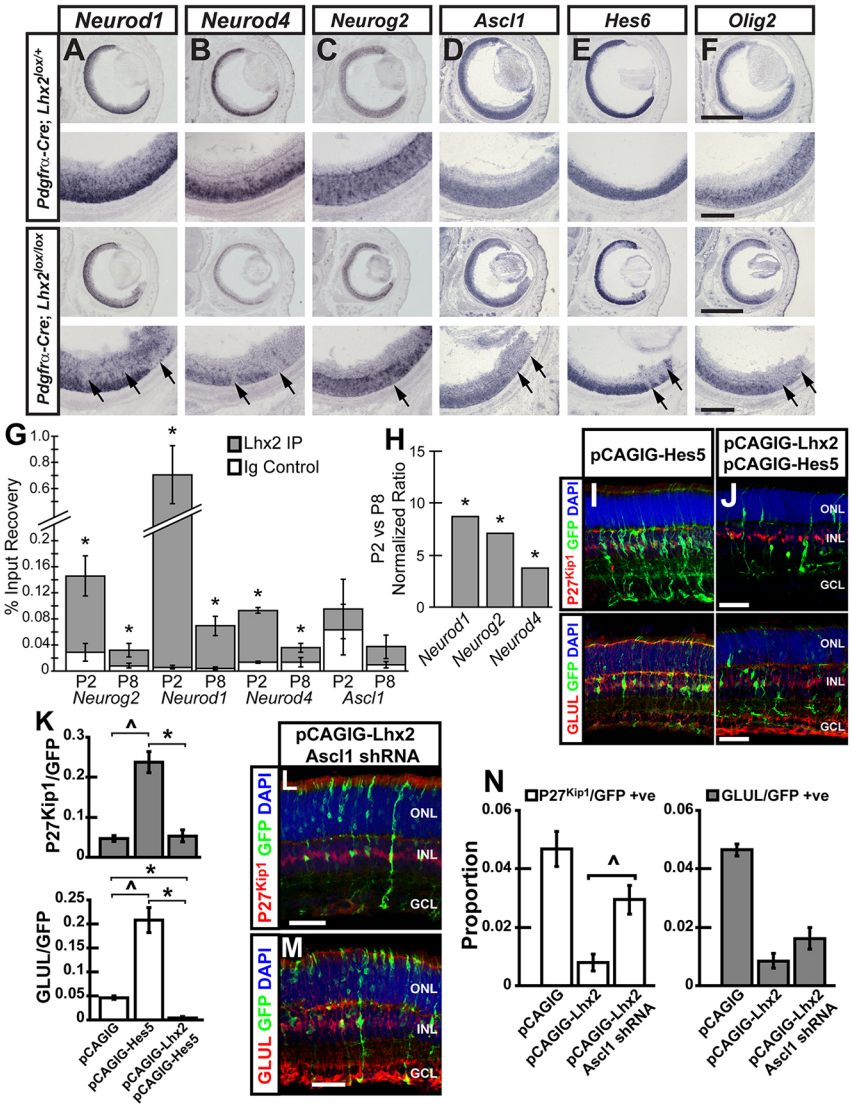

Fig. 2. *Lhx2* regulates expression of bHLH factors in the retina. (A-F) *In situ* hybridization analysis of *Lhx2*ΔcKO (*Pdgfra-Cre*; *Lhx2$^{lox/lox}$*) retinas at P0 reveals that *Lhx2* is necessary for bHLH expression. Arrows indicate loss of expression. (G) ChIP performed on retinal tissue collected at postnatal days 2 and 8. Graphs show the mean percentages of input recovery for the immunoprecipitated fractions and the isotype controls. Asterisks indicate statistical significance ($P<0.05$). Data are mean±s.e.m. (H) The normalized ratio of LHX2 binding to target loci reveals decreasing occupancy from P2 to P8. (I-K) Co-electroporation of *Lhx2* with *Hes5* blocked the gliogenic effect of *Hes5* electroporation. pCAGIG-Hes5: 23.75±2.63%, $n=6$, P27^{Kip1}; 20.83±2.46%, $n=6$, GLUL; pCAGIG-Hes5/pCAGIG-Lhx2: 5.33±1.4%, $n=6$, P27^{Kip1}; 0.43±0.1%, $n=6$, GLUL. (L-N) shRNA knockdown of *Ascl1* rescues ($P<0.05$) P27^{Kip1} expression. pCAGIG-Lhx2: 0.8±0.29%, $n=6$, P27^{Kip1}; 0.85±0.25%, $n=6$, GLUL; pCAGIG-Lhx2/Ascl1 shRNA, 2.95±0.48%, $n=6$, P27^{Kip1}; 1.62±0.36%, $n=6$, GLUL. Asterisks indicate statistical significance for G,H, but represent a significant decrease in K,N. ^ indicates a significant increase in K,N. Data are mean±s.e.m. Scale bars: 1 mm (lower magnification, A-F); 250 µm (higher magnification, A-F); 50 µm (J,L,M).

Development (2018) 145, dev159970. doi:10.1242/dev.159970

sequences located upstream of genes that contained consensus LHX2-binding sites. We found that LHX2 selectively bound to *cis*-regulatory sequences associated with the proneural bHLH genes *Neurod1*, *Neurod4* and *Neurog2* (Fig. 2G,H). Analysis of the normalized ratio of LHX2 binding at P2 versus P8 revealed increased occupancy at P2, correlating closely with the period of active neurogenesis (Fig. 2H). Intriguingly, the wfAC phenotype generated following *Lhx2* electroporation closely resembles phenotypes resulting from overexpression of the NeuroD family member *Neurod2* (Cherry et al., 2011).

Hes5 encodes an E-box-selective bHLH protein that inhibits retinal neurogenesis and promotes MG specification (Hojo et al., 2000). *Lhx2* function is required for the gliogenic effects of *Hes5* in the retina (de Melo et al., 2016a). As *Lhx2* appears to be necessary for expression of proneural bHLHs, yet is essential for *Hes5*-dependent gliogenesis, we next tested whether simultaneous misexpression of *Lhx2* and *Hes5* could promote MG specification. Electroporation of pCAGIG-Hes5 potently promoted the formation of MG (Fig. 2I,K). However, co-electroporation with pCAGIG-Lhx2 blocked the gliogenic effects of *Hes5*, and disrupted MG morphogenesis (Fig. 2J,K). The fraction of cells that expressed $P27^{Kip1}$ was similar to that of vector controls, whereas the fraction expressing GLUL was identical to that observed in retinas electroporated with *Lhx2* alone (Fig. 2K; Fig. 1D). These data indicated that *Lhx2* expression is sufficient to override the gliogenic activity of *Hes5*, and that *Hes5* cannot suppress the neurogenic properties of *Lhx2*.

Lhx2 overexpression blocks gliogenesis through an *Ascl1*-dependent mechanism, while promoting wfAC formation through *Neurog2*

The previously described data show that *Lhx2* is necessary for proneural bHLH expression. Furthermore, electroporation of *Lhx2* disrupts MG development, blocks *Hes5*-mediated MG formation, and suppresses Notch signaling in RPCs. This indicates that, although *Lhx2* is required for both Notch pathway gene expression and Notch-mediated Müller gliogenesis (de Melo et al., 2016a), misexpression of *Lhx2* in RPCs can inhibit Notch signaling and promote retinal neurogenesis, similar to the effects of overexpressing *Lhx2* in the hippocampus (Subramanian et al., 2011). One mechanism by which this might occur is through *Lhx2*-dependent regulation of the expression of *Ascl1* and *Neurog2* in RPCs, which, depending on context, can negatively (Hufnagel et al., 2010; Vasconcelos et al., 2016; Ware et al., 2016) or positively (Nelson et al., 2009) regulate Notch signaling in neural progenitors.

We first tested whether shRNA knockdown of *Ascl1* concurrent with *Lhx2* electroporation could reverse the inhibition of gliogenesis. We observed that co-electroporation of *Ascl1* shRNA constructs with pCAGIG-Lhx2 partially rescued MG differentiation, as indicated by the restoration of $P27^{Kip1}$-positive cells that display radial morphology characteristic of MG (Fig. 2L-N). Interestingly, GLUL expression remained suppressed, indicating that *Ascl1* knockdown cannot fully rescue terminal glial differentiation. In light of the partial rescue of gliogenesis, we investigated whether *Ascl1* knockdown could also reverse *Lhx2*-dependent inhibition of Notch signaling. We observed that *Ascl1* knockdown, much like misexpression of *Lhx2*, led to a modest reduction in Notch reporter expression (Fig. S3A-C,E), consistent with studies showing a dual role for *Ascl1* in both promoting Notch signaling, as well as activating expression of proneural bHLH factors in retinal progenitors (Nelson et al., 2009). However, simultaneous overexpression of *Lhx2* with knockdown of *Ascl1* leads to a dramatic reduction in Notch reporter expression (Fig. S3D,E). This is in stark contrast with the observed partial rescue of glial development (Fig. 2L-N), and indicates that rescue of Notch signaling is not the mechanism by which partial recovery of MG development occurs.

The role of *Neurog2* is less well understood in the retina, owing to its functional redundancy with *Ascl1* (Hufnagel et al., 2010). Electroporation of pCAGIG-Neurog2 at P0 was neurogenic, resulting in the specification of $PAX6^{+}$ narrow-field ACs with diffuse dendritic morphology (Fig. 3A). The population of ACs increased from 8.8% with pCAGIG to 19.8% with pCAGIG-Neurog2 (Fig. 3F). Co-electroporation of pCAGIG-Neurog2 with pCAGIG-Lhx2 yielded AC numbers that were not significantly different from controls (9.9%) (Fig. 3F). The ACs generated were wfACs with stratified dendritic morphology in layers S1, S3 and S5 of the IPL, identical to that seen following electroporation of pCAGIG-Lhx2 (Fig. 3B-E). A small fraction of these ACs were co-labeled with calretinin (CALB2) (Fig. 3B-E,I). The range of field coverage varied but was typically very large, with arbors often extending to the retinal periphery (Fig. 3C-E). We tested whether the neurogenic and wfAC phenotypes promoted by *Lhx2* required *Neurog2* by co-electroporating pCAGIG-Lhx2 with a *Neurog2* shRNA construct. We found that knockdown of *Neurog2* expression completely blocked the formation of wfACs, as shown by the disappearance of the distinct stratified arborization pattern but continued presence of ACs (Fig. 3G,H, arrows). However, in contrast to knockdown of *Ascl1*, *Neurog2* knockdown did not rescue the disruption of MG development that resulted from *Lhx2* overexpression (Fig. 3H).

The neurogenic role of *Lhx2* is mediated by interaction with *Ldb1*, but the *Lhx2* co-factor *Rnf12* activates *Lhx2*-dependent gliogenesis

The LIM domain-binding protein LDB1 directly interacts with LHX2 (Bach et al., 1999). Recent studies of LDB function in early-stage RPCs have shown that loss of function of either *Ldb1* or *Ldb2* does not affect RPC proliferation or gliogenesis, but loss of function of both *Ldb1* and *Ldb2* genes phenocopies the loss of function of *Lhx2* (Gueta et al., 2016). We found that *Ldb1* mRNA expression is broadly expressed in the developing retina, being readily detectable in RPCs in the retinal neuroblastic layer (NBL), and in differentiated neurons (Fig. S4). Expression becomes localized primarily to ganglion cell layer (GCL) and inner nuclear layer (INL) cells in the mature retina (Fig. S4F″,G″). Co-expression of *Ldb1* and *Lhx2* mRNA is observed in RPCs in the NBL from E14 to P2, and in INL cells from P5 to P21 (Fig. S4). Because of this overlap of expression of *Ldb1* and *Lhx2*, we tested whether electroporation of *Ldb1* could modify the developmental effects induced by *Lhx2* overexpression.

Electroporation of pCAGIG-Ldb1 resulted in a significant decrease in the production of MG, from 4.7% $P27^{Kip1+}$ and 4.7% $GLUL^{+}$ in control electroporated cells, to 2.1% and 2.0%, respectively (Fig. 4A,B,I). The reduction was less pronounced than that observed following electroporation with pCAGIG-Lhx2 and, unlike *Lhx2* electroporation, no notable changes in AC morphology were observed (Fig. 4A,B; Fig. S5). Outside of the reduction in MG, no significant changes in the patterns or morphology of electroporated cells could be distinguished between pCAGIG and pCAGIG-Ldb1 (Fig. 4A,B; Fig. S5). Co-electroporation of pCAGIG-Lhx2 with pCAGIG-Ldb1 produced a phenotype identical to that observed in *Lhx2* electroporations: a significant loss of MG and production of wfACs (Fig. 4C,D,I; Fig. S5).

Development (2018) 145, dev159970. doi:10.1242/dev.159970

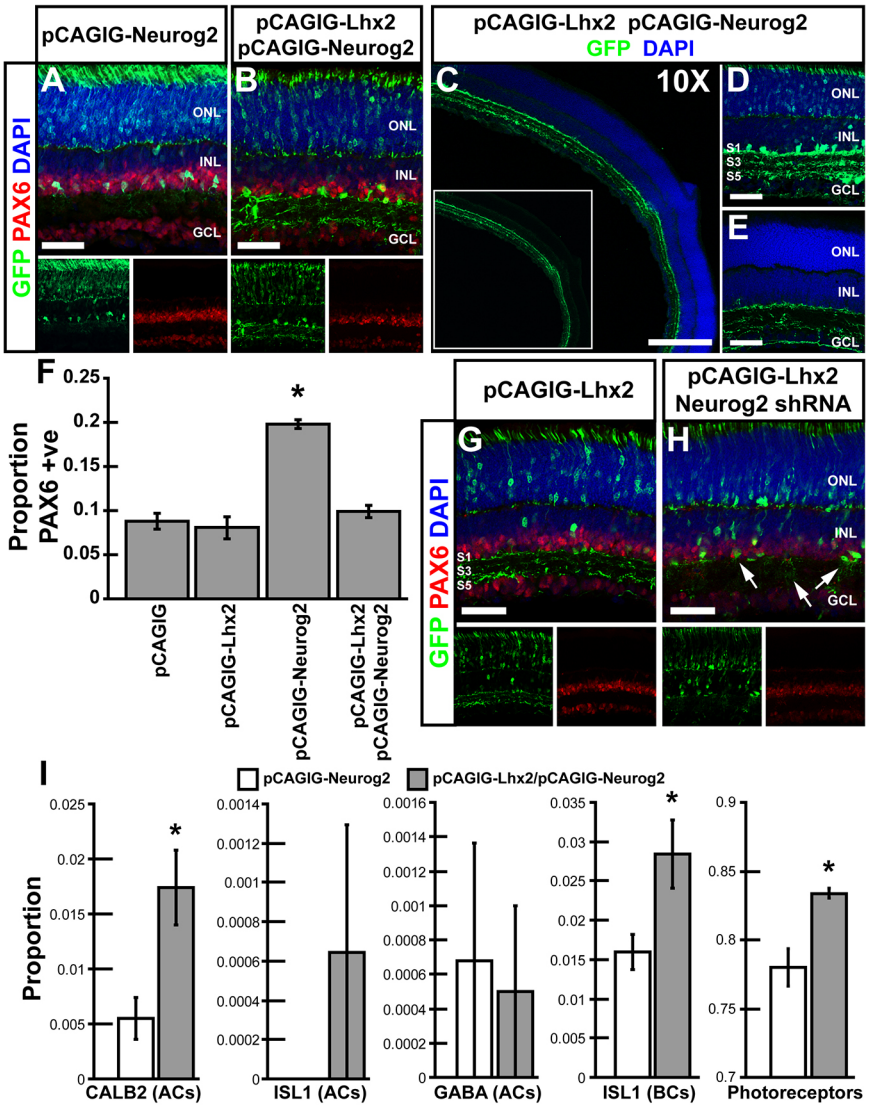

Fig. 3. *Lhx2* synergistically promotes the formation of wide-field amacrine cells with *Neurog2*. (A,F) Electroporation of *Neurog2* results in an increase in the formation of narrow-field diffusely arborizing amacrine cells. (B,F) Co-electroporation of *Lhx2* with *Neurog2* transforms the morphology of ACs from narrow-field diffusely arborizing to wide-field selectively stratified. The overall fraction of ACs is unchanged relative to pCAGIG-Lhx2 or pCAGIG electroporated retinas. (C-E) Electroporation of *Lhx2* with *Neurog2* results in a synergistic expansion of the width of the dendritic field. (G,H) shRNA-mediated knockdown of *Neurog2* blocks the formation of wide-field amacrine cells generated by electroporation of *Lhx2*. (H, arrows) The lateral S1, S3, and S5 stratified dendritic arbors are lost. (I) Co-electroporation of *Lhx2* with *Neurog2* results in significant increases in the number of CALB2^{+} amacrine cells (primarily AII), bipolar cells and photoreceptors compared with electroporation of *Neurog2* alone (P<0.05). S, inner plexiform layer sublamina. Scale bars: 50 µm in A,B,D,E,G,H; 200 µm in C.

We also investigated the effects of loss of LDB function by overexpressing a dominant-negative (DN) construct of Ldb1, which has previously been shown to phenocopy loss of *Lhx2* function in hippocampal progenitors (Subramanian et al., 2011). We observed that overexpression of DN-LDB1 in P0 retina phenocopies the previously described loss of function of *Lhx2* (de Melo et al., 2016a), resulting in a loss of MG, but not in the fraction of BCs or photoreceptors (Fig. S6). These results confirmed that LDB factors are indeed necessary for *Lhx2*-mediated regulation of RPC maintenance and gliogenesis.

As developmental outcomes mediated by LIM-HD factors, including LHX2, are co-regulated by *Rnf12* (Ostendorff et al., 2002; Hiratani et al., 2003), we tested whether *Rnf12* expression could alter *Lhx2* function in the retina. Analysis of *Rnf12* mRNA expression in the developing retina revealed relatively low expression in RPCs from E14 to E18 timepoints (Fig. S4A′-C′) compared with the enriched expression observed at postnatal timepoints (Fig. S4D′-F′). Postnatal expression revealed a distinct upregulation and enrichment of RNA expression in subsets of cells in the NBL from P0 to P2 and in the medial INL at P5, consistent with the spatial and temporal onset of Müller gliogenesis (Fig. S4D′-F′), as well as with previous studies that reported increased expression of *Rnf12* during differentiation of MG precursors (Nelson et al., 2011).

Electroporation of pCAGIG-Rnf12 at P0 led to a significant increase in the production of MG from 4.7% and 4.6% (P27^{Kip1+} and GLUL^{+}, respectively) in controls, to 7.72% and 8.3% (Fig. 4E,F, arrows and Fig. 4J). Furthermore, co-electroporation of *Rnf12* with *Lhx2* rescued the reduction in gliogenesis observed following electroporation of *Lhx2* alone (Fig. 4G,H, arrows and Fig. 4J). We also observed that co-electroporation of *Rnf12* with *Lhx2* reversed the observed changes in amacrine cell morphology that resulted from *Lhx2* electroporation, preventing the formation of wfACs (Fig. 4G,H; Fig. S5F). Electroporation of *Rnf12* alone or with *Lhx2* inhibited the formation of ACs broadly (Fig. S5E-G). We next tested whether *Rnf12* was required for glial development. Electroporation with shRNA constructs targeting *Rnf12* at P0 resulted in a loss of MG as determined by P27^{Kip1} and GLUL immunostaining (Fig. 4K,L, arrows; Fig. 4M-O). The relative loss of MG was nearly identical to that reported following *Lhx2* loss of function (de Melo et al., 2016a). To determine whether *Rnf12* requires *Lhx2* in order to promote MG differentiation, we co-electroporated pCAGIG-Rnf12 with pCAG-Cre into *Lhx2*$^{+/+}$ and *Lhx2*$^{lox/lox}$ retinas at P0. Concurrent loss of function of *Lhx2* blocked

Development (2018) 145, dev159970. doi:10.1242/dev.159970

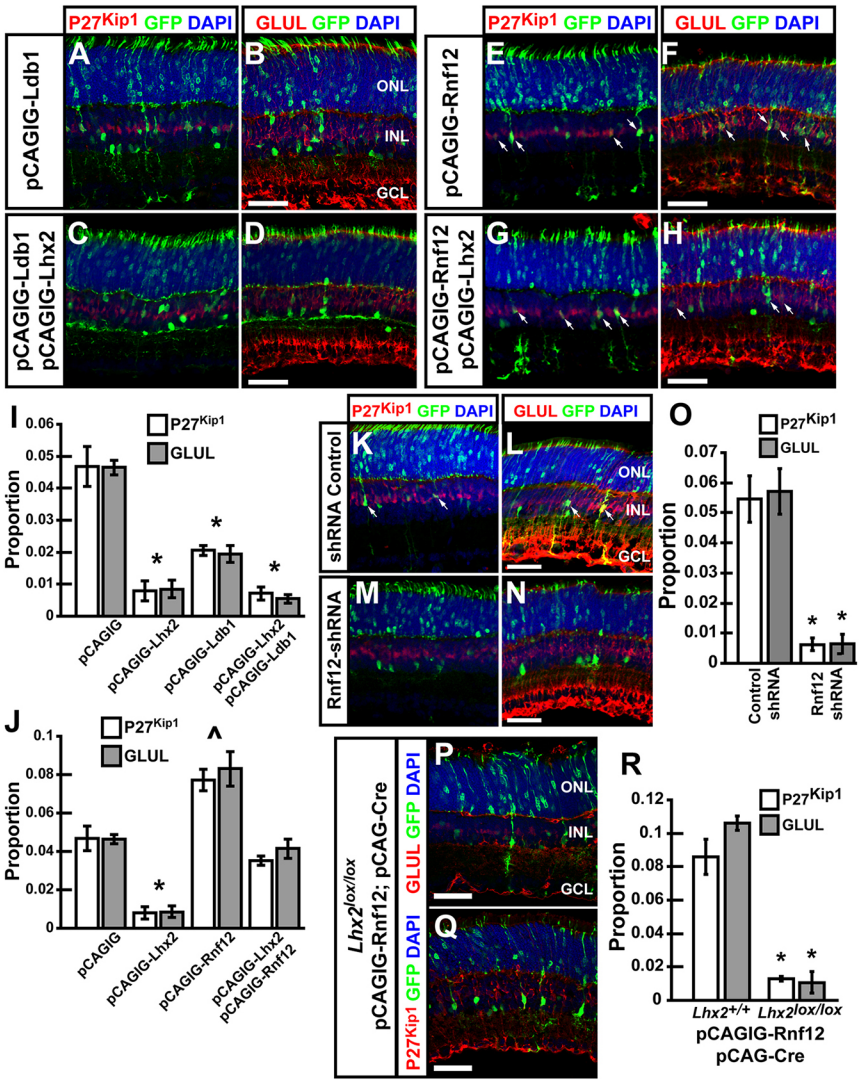

Fig. 4. Co-electroporation of *Lhx2* with *Ldb1* or *Rnf12* differentially affects Müller gliogenesis.
(A-D,I) Electroporation of *Ldb1* inhibits the formation of MG, and co-electroporation of *Lhx2* with *Ldb1* generates an identical phenotype to electroporation of *Lhx2* alone. (E-H, arrows, J) Electroporation of *Rnf12* significantly increases the proportion of MG generated (7.73±0.53%, n=6, $P27^{Kip1}$ and 8.3±0.85%, n=6, GLUL), while co-electroporation of *Lhx2* with *Rnf12* rescues MG (3.53±0.19%, n=6, $P27^{Kip1}$ and 4.15±0.45%, n=6, GLUL). (K,L arrows; M-O) shRNA knockdown of *Rnf12* significantly blocks the formation of MG compared with shRNA controls (5.45±0.75%, n=6, $P27^{Kip1}$ and 5.72±0.74%, n=6, GLUL versus 0.63±0.18%, n=6, $P27^{Kip1}$ and 0.64±0.31%, n=6, GLUL). (P-R) *Rnf12* requires functional *Lhx2* to promote MG development: (P<0.05; n=3) $P27^{Kip1}$ and (P<0.05; n=3) GLUL. Asterisks indicate significant decreases. ^Significant increase. Data are mean±s.e.m. Scale bars: 50 µm.

the *Rnf12*-dependent increase in gliogenesis (Fig. 4P-R). In these mice, the proportion of $P27^{Kip1}$ and $GLUL^{+}$ electroporated cells (1.3% and 1.1%, respectively) was nearly identical to that reported following *Lhx2* loss of function (de Melo et al., 2016a). Taken together, these results suggest that *Rnf12* acts through an *Lhx2*-dependent mechanism in late-stage RPCs to induce gliogenesis.

Misexpression of *Lhx2*/*Ldb1* or *Rnf12* does not result in altered mRNA levels of proneural or proglial bHLH factors

We have demonstrated that *Lhx2* is necessary for expression of multiple proneural bHLH factors in RPCs (Fig. 2A-F, Table S1). LHX2 directly binds to putative *cis*-regulatory elements associated with these genes (Fig. 2G,H), and the effects of overexpression of *Lhx2* are disrupted by knockdown of *Ascl1* and *Neurog2* (Figs 2L-N and 3G,H). We therefore investigated whether overexpression of *Lhx2* and *Ldb1* directly resulted in increased mRNA levels of these genes, relative to pCAGIG alone or to *Rnf12* overexpression. Surprisingly, when conducting qRT-PCR analysis of cells isolated 36 h after electroporation, we did not observe significant changes in mRNA levels for any of the bHLH factors tested, despite the fact that robust expression of vector-derived *Lhx2*, *Ldb1* and/or *Rnf12* are all detected at this stage (Fig. S7).

Lower relative levels of LHX2-LDB1 protein complexes are seen as gliogenesis is initiated

We have previously shown that LHX2 interacts with LDB1 in developing retina at E15.5 and P0.5 (Gueta et al., 2016). The findings in this study suggest that upregulation of *Rnf12* may lead to the relative fraction of LHX2 bound to LDB1 decreasing during gliogenesis due to RNF12-dependent degradation of LDB1. To test this hypothesis, we performed immunoprecipitation analysis of LHX2 and LDB1 at three different timepoints. We analyzed LHX2 protein complexes at E16, when only neurons are born, at P2, when gliogenesis is beginning, and at P5, when gliogenesis peaks (Young, 1985). Both LHX2 and LDB1 were expressed and directly interacted with one another at all three stages (Fig. 5A). However, when immunoprecipitation was performed with antibodies to LHX2, levels of recovered LDB1 levels showed a substantial reduction at P2 relative to E16, and even more pronounced reductions at P5 (Fig. 5B), when normalized to total levels of immunoprecipitated LHX2.

DISCUSSION

The molecular mechanisms that control CNS gliogenesis are still poorly understood. Work from many groups has shown that a combination of genes encoding extrinsic and intrinsic signals

Development (2018) 145, dev159970. doi:10.1242/dev.159970

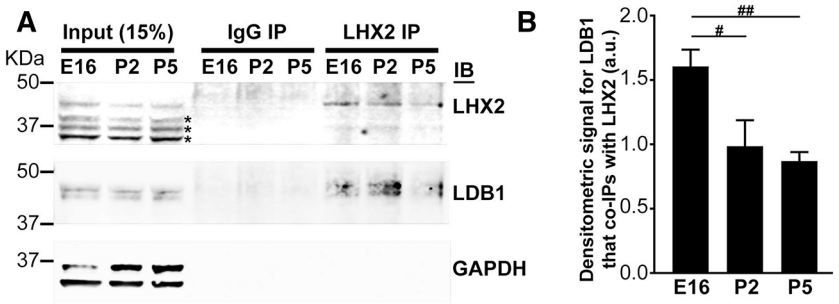

Fig. 5. Reduced levels of the LHX2-LDB1 are seen following the onset of retinal gliogenesis. (A) Co-immunoprecipitation of LDB1 with LHX2 in retinal tissue collected at E16, P2 and P5. Decreased LDB1 interaction with LHX2 is observed at P5. IgG immunoprecipitation is used as negative control. Asterisks indicate non-specific bands detected using the anti-LHX2 antibody that do not appear in immunoprecipitation lanes. (B) One-way ANOVA of the densitometry signals of LDB1 that co-immunoprecipitate with LHX2 at each timepoint indicated a significant increase (P=0.0016). The relative levels of LDB1 recovered following immunoprecipitation using anti-LHX2 antibodies following normalization to the total amount of LHX2 protein in the input lane. This controls for developmental changes in LHX2 levels. Post-hoc t-test indicates that the decrease in levels of LDB1 that co-immunoprecipitate with LHX2 decrease significantly over time (E16>P2>P5). $^{\#}P$=0.016 and $^{\#\#}P$=0.003 (post-hoc t-test).

control gliogenesis. Extrinsic signals include the Notch/Delta pathway, whereas several transcription factors, including *Sox9*, *Nfia*, *Hes5* and *Zbtb20*, have been shown to be either necessary or sufficient to induce gliogenesis (Hojo et al., 2000; Kang et al., 2012; Nagao et al., 2016).

Here, we shed light on the mechanism by which context-specific functions of *Lhx2* are regulated during retinal development. In this study, we confirm and extend previous work that demonstrated an essential role for *Ldb1-Lhx2* function in both RPC proliferation and retinal gliogenesis. We show that ectopic *Lhx2* expression potently suppresses Notch signaling, resulting in early RPC cell cycle exit and blocking retinal gliogenesis, while at the same time promoting formation of wfACs. The formation of wfACs was further enhanced by ectopically co-expressing *Lhx2* with *Neurog2*, resulting in more expansive lateral arborization and co-expression of the AC marker CALB2. Conversely, co-electroporation of *Lhx2* with a *Neurog2* shRNA blocked wfAC formation. These results indicate that concurrent activation of pro-neural *Neurog2* function may be required for the complete instructive wfAC effects of *Lhx2*. We further demonstrate that these effects are dependent on *Ascl1* and *Neurog2*, respectively. We also show that *Rnf12*, which specifically ubiquitylates LDB proteins and targets them for proteolysis, is both necessary and sufficient to promote Müller glial development, and does so in a strictly *Lhx2*-dependent manner. Upregulation of *Rnf12* expression correlated with a reduction in retinal levels of the LHX2-LDB1 complex, concurrent with the onset and progression of gliogenesis.

These findings highlight the importance of LIM co-factor-mediated *Lhx2*-dependent transcriptional activation in controlling cell fate specification in the CNS. This does not, however, exclude a parallel function of *Rnf12* in promoting *Lhx2*-dependent transcriptional repression. Although *Lhx2*-dependent transcriptional activation is dependent on LDB proteins, *Lhx2*-dependent transcriptional repression involves recruitment of histone modifying enzymes, including the HDAC and NuRD protein complexes (Bach et al., 1999; Muralidharan et al., 2017). RNF12 itself can directly bind both LHX2 and SIN3A, leading to recruitment of HDAC proteins (Bach et al., 1999). It is thus possible that *Rnf12* may promote gliogenesis by both attenuating *Lhx2*/*Ldb1*-dependent activation of proneural genes, and by triggering *Lhx2*-dependent repression of these genes.

The precise identity of these genes, however, remains unclear. We and others have shown that LHX2 regulates expression of multiple Notch pathway genes (de Melo et al., 2016a), and that this is of central importance to actively regulating the balance of neurogenesis and gliogenesis in RPCs. In this study, we also show that *Lhx2* regulates expression of Notch-regulated bHLH factors – such as *Ascl1*, *Neurog2* and *Hes6*, as well as multiple Notch-independent proneural bHLH factors, such as members of the *NeuroD* family (Morrow et al., 1999; Jadhav et al., 2006). *NeuroD* family genes in turn induce wfAC formation when overexpressed (Cherry et al., 2011). We also demonstrate that neurogenesis and wfAC formation induced by misexpression of *Lhx2* are both blocked by knockdown of *Ascl1* and *Neurog2*, respectively. Although this suggested that overexpression of *Lhx2* might inhibit Notch signaling, while enhancing neurogenesis and wfAC formation by stimulating transcription of proneural bHLH factors, this proved not to be the case. It appears that misexpression of *Lhx2* may regulate these processes through presently uncharacterized target genes and/or by regulating the activity or function of proneural bHLH factors through as yet unknown mechanisms. Identifying precisely how *Lhx2* regulates neurogenesis, Notch signaling and wfAC formation will be an important topic for future studies.

In both the retina and other CNS regions, *Lhx2* acts as a selector gene that simultaneously activates and represses different sets of tissue and/or state-specific genes. In early-stage RPCs, *Lhx2* simultaneously activates expression of RPC-specific genes, while suppressing genes that are specific to anterodorsal hypothalamus and thalamic eminence (Roy et al., 2013). Likewise, in early cortical progenitors, *Lhx2* activates cortical plate-specific genes, while repressing expression of genes enriched within the cortical hem (Mangale et al., 2008). The dynamic regulation of *Rnf12* and *Ldb* activity, which plays a central role in control of retinal cell fate, may also be important for these selector functions of *Lhx2*.

MATERIALS AND METHODS

Animals

Timed pregnant CD-1 mice used for *in situ* hybridization, electroporation and ChIP were purchased from Charles River Laboratories. Mice were housed in a climate-controlled pathogen-free facility, on a 12 h/12 h light/dark cycle (08:00, lights on; 20:00, lights off). *Pdgfrα-Cre* (stock #013148) mice were purchased from the Jackson Laboratory while *Lhx2*$^{lox/lox}$ mice were obtained from Dr Edwin Monuki (University of California, Irvine, USA). *Lhx2*$^{lox/lox}$; *Pdgfrα-Cre* and *Lhx2*$^{+/+}$; *Pdgfrα-Cre* mice were bred and maintained in the lab as previously described (de Melo et al., 2016a). All experimental procedures were preapproved by the Institutional Animal Care and Use Committee of the Johns Hopkins University School of Medicine.

Development (2018) 145, dev159970. doi:10.1242/dev.159970

Cell counts

All counts were made blinded on whole retinal sections or on dissociated retinas as previously described (de Melo et al., 2012, 2016a). Differences between the two means were assessed using an unpaired two-tailed Student's *t*-test.

Chromatin immunoprecipitation

zCD-1 mice were sacrificed at postnatal day (P) 2 and P8 according to Johns Hopkins IACUC animal policies. ChIP was performed as previously described (de Melo et al., 2016a). Whole dissected retinas were dissociated in a collagenase I suspension, crosslinked in 1% formaldehyde, quenched in 125 mM glycine and the extracted nuclei were sheared to produce 100 to 500 bp fragments by means of probe sonication. Chromatin was immunoprecipitated by using goat anti-Lhx2 antibody (Santa Cruz Biotechnology) or the related isotype control (Abcam), retained on agarose beads (Invitrogen), and washed and purified by organic extraction. Candidate target genes demonstrating altered expression levels in *Lhx2* conditional knockout retinas by RNA-seq were screened for LHX2 consensus binding sites within annotated regulatory regions by querying the JASPAR repository database (Mathelier et al., 2016), and was based on GSE48068 (Folgueras et al., 2013). Computationally inferred Lhx2-binding sites and proximal negative control regions were analyzed in ChIP-enriched fractions and isotype controls by SYBR-qPCR (Agilent Technologies).

Electroporation

For *in vivo* electroporation experiments, retinas were electroporated at P0 as previously described, and harvested for analysis at P1, P2 or P14 subject to the requirements of the study. DNA constructs used for gene misexpression in this study are as follows: pCAGIG (Addgene plasmid 11159, deposited by C. Cepko and modified into a Gateway destination vector in lab), pCAGIG-Hes5 [Gateway cloned from Ultimate Human ORF Collection (Life Technologies)], pCAGIG-Ldb1 [Gateway cloned from Ultimate Human ORF Collection (Life Technologies)], pCAGIG-Lhx2 [Gateway cloned from Ultimate Human ORF Collection (Life Technologies)], pCAGIG-Ngn2 (NeuroG2) [Gateway cloned from Ultimate Human ORF Collection (Life Technologies)], pCAGIG-Rnf12 [Gateway cloned from Ultimate Human ORF Collection (Life Technologies)], pCAGIG-CD4 [Gateway cloned from Ultimate Human ORF Collection (Life Technologies)]. DNA constructs used for Notch reporter analysis in this study are as follows: pCAG (modified from pCAGIG), pCAG-DsRed (Addgene plasmid 11151, deposited by C. Cepko), pCAG-Lhx2 [Gateway cloning from Ultimate Human ORF Collection (Life Technologies)], pCBFRE-GFP (Addgene plasmid 17705, deposited by N. Gaiano). DNA constructs used for shRNA knockdown in this study are as follows: Ascl1 shRNA (clone TRCN0000075398, TRC-Open Biosystems), Rnf12 shRNA (clone TRCN0000095740, TRC-Open Biosystems), Ngn2 (Neurog2) shRNA (clone FP-301 obtained from Franck Polleux, Columbia University, NY, USA) (Root et al., 2006; Hand and Polleux, 2011), and control (pLKO.1 vector control, TRC-Open Biosystems). All shRNA constructs have been previously shown to give substantial (>70%) knockdown of their target gene. DNA constructs used for Lhx2 loss of function in this study are as follows: pCAG-Cre (Addgene plasmid 13775, deposited by C. Cepko) and pCALNL-GFP (Addgene plasmid 13770, deposited by C. Cepko).

For *ex vivo* electroporation studies, eyes were enucleated from P0 animals and placed in ice-cold PBS. The cornea and scleral/RPE tissue was dissected off of the retinas, leaving the retina, iris and lens. Retinas were placed in a custom chamber containing 1 µg/µl in PBS of all DNA constructs to be electroporated in a given experiment, positioning the apical retina towards the negative pole. Electroporation occurred after 5-50 mV; 50 ms square-wave pulses from a BTX ECM830 square-wave electroporator (Harvard Apparatus). Upon electroporation, the iris and lens was dissected from the retina, and retinas were flat mounted on 0.2 µm Nuclepore Track-Etch Membranes (Whatman) such that the apical retina was placed onto the filter. Explants were then placed in suspension culture in DMEM supplemented with 10% FBS and 100 U/ml penicillin/streptomycin for 36 h.

Quantitative real-time PCR

Retinas were electroporated at P0 with multiple constructs together with pCAGIG-CD4. Explants were harvested 36 h later and dissociated, and the electroporated cells were isolated using Dynabeads conjugated with anti-human CD4 (Thermo-Fisher). qRT-PCR was performed as previously described (de Melo et al., 2016a), with signals normalized to *Gapdh*. Primers used are listed in Table S2.

Immunohistochemistry

Antibodies used for fluorescent immunohistochemistry are as follows: goat anti-Brn3 (1:200; Santa Cruz Biotechnology), mouse anti-calbindin (Calb1) (1:200; Sigma-Aldrich), rabbit anti-calretinin (Calb2) (1:200; Chemicon), goat anti-Chat (1:100; Chemicon), sheep anti-Chx10 (Vsx2) (1:200; Exalpha Biologicals), rabbit anti-Dab1 (1:200; EMD Millipore), rabbit anti-DsRed (1:500; Clontech Laboratories), rabbit anti-GABA (1:200; Sigma), mouse anti-Gad6 (Gad2) (1:200; Developmental Studies Hybridoma Bank, University of Iowa), goat anti-GFP (1:500; Rockland Immunochemicals), rabbit anti-GFP (1:1000; Invitrogen), mouse anti-glutamine synthase (Glul) (1:200; BD Biosciences), rat anti-glycine (1:200; ImmunoSolution), mouse anti-islet1 (1:200; Developmental Studies Hybridoma Bank), mouse anti-Ki67 (1:200; BD Biosciences), rabbit anti-Lhx2 (1:1500; generated in-house with Covance), mouse anti-P27 (1:200; Invitrogen), mouse anti-Pax6 (1:200; Developmental Studies Hybridoma Bank), rabbit anti-TH (1:500; Pel Freez) and mouse anti-VGlut3 (1:200; Antibodies Incorporated). Secondary antibodies used were FITC-conjugated donkey anti-goat IgG (1:500; Jackson Immunoresearch), FITC-conjugated donkey anti-mouse IgG (1:500; Jackson Immunoresearch), FITC-conjugated donkey anti-rabbit IgG (1:500; Jackson Immunoresearch), Texas Red-conjugated donkey anti-goat IgG (1:500; Jackson Immunoresearch), Texas Red-conjugated donkey anti-mouse IgG (1:500; Jackson Immunoresearch), Texas Red-conjugated donkey anti-rabbit IgG (1:500; Jackson Immunoresearch) and Texas Red-conjugated donkey anti-sheep IgG (1:500; Jackson Immunoresearch). All section immunohistochemical data shown was imaged and photographed on a Zeiss Meta 510 LSM confocal microscope.

In situ hybridization

Single-color *in situ* hybridization was performed as previously described (Blackshaw, 2013). RNA probes were generated using the following EST sequences as templates: *Ascl1*, GenBank accession number BE953927; *Hes6*, GenBank accession number AW048812; *Neurod1*, GenBank accession number AI835157; *Neurod4*, GenBank accession number AI846749, *Neurog2*, GenBank accession number BC055743; and *Olig2*, GenBank accession number AI844033.

Immunoblotting and immunoprecipitation

Wild-type retinal tissues were harvested from E16 (eight litters), P2 (five litters) and P5 (five litters), and snap-frozen for storage. After pooling tissues from all litters, tissue homogenization was carried out by aspirating the tissue 20 times using a 23-gauge needle in lysis buffer (100 mM Tris-HCl, 150 mM NaCl, 25 mM NaF,50 µM $ZnCl_2$, 15% glycerol, 1% Triton X-100) supplemented with protease inhibitors (Roche #11697498001) and BitNuclease (Biotools #B16003) for clarification. Following a 1 h incubation at 4°C, supernatant were collected after centrifuging at 8200 ***g*** for 10 min at 4°C. Following normalization using standard BCA assay, immunoprecipitation was carried out by first incubating lysates overnight at 4°C with 5 µg of anti-LHX2 (clone ID: R911.1.2E3, CDI Labs, #15-389) and mouse pan-IgG (#sc-2025, Santa Cruz), respectively. Next, the antibody-protein complexes were pulled down by incubating for 2 h with ProteinG Dynabeads (ThermoFisher #10004D) at 4°C, washed thrice with lysis buffer and eluted in LDS-sample loading buffer (ThermoFisher #NP0008). Input lysate along with the immunoprecipitate samples were resolved in a SDS-PAGE gel and immunoblotted sequentially using anti-LHX2 (1:750, clone ID: R911.1.2E3, CDI Labs, #15-389), LDB1 (1:1000; Sigma, #HPA034488) and GAPDH (Sigma, #G8795) antibodies. Anti-rabbit IRDye680RD (LiCor, #925-68071) and light-chain-specific anti-mouse AlexaFluor 790 (Jackson Immunolabs, #115-655-174) secondary antibodies were used to

visualize bands, and blots were imaged using an infra-red fluorescence imager (LiCor Clx).

Densitometry and statistical analysis

Three technical repeats of the co-immunoprecipitation experiments were performed, followed by three independent immunoblots. Densitometry signal from lanes corresponding to LHX2 input, LHX2 immunoprecipitation, LDB1 immunoprecipitation and GADPH loading controls of all three SDS-PAGE gels was measured using LiCor image studio software. Following normalization of signal from LHX2 immunoprecipitation to its respective input, the ratio of LDB1 co-immunoprecipitation with LHX2 was calculated. Statistical analysis was performed using R software. We performed linear regression (r, lm) to adjust batch effects in the ratio of LDB1 co-immunoprecipitation with LHX2 between the three blots. Next, we performed one-way ANOVA (r, aov) using the adjusted values to test if there were any statistically significant differences between the means of LDB1 signal that co-immunoprecipitated with LHX2 in the E16, P2 and P5 samples. For post-hoc pairwise comparisons, we performed a *t*-test (r, *t*-test).

Acknowledgements

We thank K. Yang for help with statistical analysis and W. Yap for comments on the manuscript.

Competing interests

The authors declare no competing or financial interests.

Author contributions

Conceptualization: J.d.M., S.B.; Methodology: J.d.M., A.V., S.B.; Validation: J.d.M., A.V., C.Z., B.S.C., F.S.; Formal analysis: J.d.M., A.V., C.Z., B.S.C., F.S.; Investigation: J.d.M., A.V., C.Z., B.S.C., F.S.; Data curation: J.d.M.; Writing - original draft: J.d.M., S.B.; Writing - review & editing: J.d.M., S.B.; Supervision: S.B.; Project administration: S.B.; Funding acquisition: S.B.

Funding

This study was supported by grants from the National Institutes of Health to B.S.C. (F32EY024201, K99EY027844) and S.B. (R01EY020560). Deposited in PMC for release after 12 months.

Data availability

RNA-seq data analyzed in this study are publicly available in GEO under accession number GSE75889.

Supplementary information

Supplementary information available online at
http://dev.biologists.org/lookup/doi/10.1242/dev.159970.supplemental

References

Artavanis-Tsakonas, S., Rand, M. D. and Lake, R. J. (1999). Notch signaling: cell fate control and signal integration in development. *Science* **284**, 770-776.

Bach, I., Rodriguez-Esteban, C., Carriere, C., Bhushan, A., Krones, A., Rose, D. W., Glass, C. K., Andersen, B., Izpisua Belmonte, J. C. and Rosenfeld, M. G. (1999). RLIM inhibits functional activity of LIM homeodomain transcription factors via recruitment of the histone deacetylase complex. *Nat. Genet.* **22**, 394-399.

Balasubramanian, R., Bui, A., Ding, Q. and Gan, L. (2014). Expression of LIM-homeodomain transcription factors in the developing and mature mouse retina. *Gene Expr. Patterns* **14**, 1-8.

Becker, T., Ostendorff, H. P., Bossenz, M., Schlüter, A., Becker, C. G., Peirano, R. I. and Bach, I. (2002). Multiple functions of LIM domain-binding CLIM/NLI/Ldb cofactors during zebrafish development. *Mech. Dev.* **117**, 75-85.

Blackshaw, S. (2013). High-throughput RNA in situ hybridization in mouse retina. *Methods Mol. Biol.* **935**, 215-226.

Cherry, T. J., Wang, S., Bormuth, I., Schwab, M., Olson, J. and Cepko, C. L. (2011). NeuroD factors regulate cell fate and neurite stratification in the developing retina. *J. Neurosci.* **31**, 7365-7379.

Chou, S.-J. and O'Leary, D. D. M. (2013). Role for Lhx2 in corticogenesis through regulation of progenitor differentiation. *Mol. Cell. Neurosci.* **56**, 1-9.

de Melo, J., Miki, K., Rattner, A., Smallwood, P., Zibetti, C., Hirokawa, K., Monuki, E. S., Campochiaro, P. A. and Blackshaw, S. (2012). Injury-independent induction of reactive gliosis in retina by loss of function of the LIM homeodomain transcription factor Lhx2. *Proc. Natl. Acad. Sci. USA* **109**, 4657-4662.

de Melo, J., Clark, B. S. and Blackshaw, S. (2016a). Multiple intrinsic factors act in concert with Lhx2 to direct retinal gliogenesis. *Sci. Rep.* **6**, 32757.

de Melo, J., Zibetti, C., Clark, B. S., Hwang, W., Miranda-Angulo, A. L., Qian, J. and Blackshaw, S. (2016b). Lhx2 is an essential factor for retinal gliogenesis and notch signaling. *J. Neurosci.* **36**, 2391-2405.

Folgueras, A. R., Guo, X., Pasolli, H. A., Stokes, N., Polak, L., Zheng, D. and Fuchs, E. (2013). Architectural niche organization by LHX2 is linked to hair follicle stem cell function. *Cell Stem Cell* **13**, 314-327.

Gordon, P. J., Yun, S., Clark, A. M., Monuki, E. S., Murtaugh, L. C. and Levine, E. M. (2013). Lhx2 balances progenitor maintenance with neurogenic output and promotes competence state progression in the developing retina. *J. Neurosci.* **33**, 12197-12207.

Gueta, K., David, A., Cohen, T., Menuchin-Lasowski, Y., Nobel, H., Narkis, G., Li, L., Love, P., de Melo, J., Blackshaw, S., et al. (2016). The stage-dependent roles of Ldb1 and functional redundancy with Ldb2 in mammalian retinogenesis. *Development* **143**, 4182-4192.

Hand, R. and Polleux, F. (2011). Neurogenin2 regulates the initial axon guidance of cortical pyramidal neurons projecting medially to the corpus callosum. *Neural Dev.* **6**, 30.

Hiratani, I., Yamamoto, N., Mochizuki, T., Ohmori, S. Y. and Taira, M. (2003). Selective degradation of excess Ldb1 by Rnf12/RLIM confers proper Ldb1 expression levels and Xlim-1/Ldb1 stoichiometry in Xenopus organizer functions. *Development* **130**, 4161-4175.

Hojo, M., Ohtsuka, T., Hashimoto, N., Gradwohl, G., Guillemot, F. and Kageyama, R. (2000). Glial cell fate specification modulated by the bHLH gene Hes5 in mouse retina. *Development* **127**, 2515-2522.

Huang, C., Chan, J. A. and Schuurmans, C. (2014). Proneural bHLH genes in development and disease. *Curr. Top. Dev. Biol.* **110**, 75-127.

Hufnagel, R. B., Le, T. T., Riesenberg, A. L. and Brown, N. L. (2010). Neurog2 controls the leading edge of neurogenesis in the mammalian retina. *Dev. Biol.* **340**, 490-503.

Jadhav, A. P., Cho, S.-H. and Cepko, C. L. (2006). Notch activity permits retinal cells to progress through multiple progenitor states and acquire a stem cell property. *Proc. Natl. Acad. Sci. USA* **103**, 18998-19003.

Kang, P., Lee, H. K., Glasgow, S. M., Finley, M., Donti, T., Gaber, Z. B., Graham, B. H., Foster, A. E., Novitch, B. G., Gronostajski, R. M. et al. (2012). Sox9 and NFIA coordinate a transcriptional regulatory cascade during the initiation of gliogenesis. *Neuron* **74**, 79-94.

Mangale, V. S., Hirokawa, K. E., Satyaki, P. R. V., Gokulchandran, N., Chikbire, S., Subramanian, L., Shetty, A. S., Martynoga, B., Paul, J., Mai, M. V. et al. (2008). Lhx2 selector activity specifies cortical identity and suppresses hippocampal organizer fate. *Science* **319**, 304-309.

Mathelier, A., Fornes, O., Arenillas, D. J., Chen, C.-Y., Denay, G., Lee, J., Shi, W., Shyr, C., Tan, G., Worsley-Hunt, R. et al. (2016). JASPAR 2016: a major expansion and update of the open-access database of transcription factor binding profiles. *Nucleic Acids Res.* **44**, D110-D115.

Matthews, J. M., Bhati, M., Craig, V. J., Deane, J. E., Jeffries, C., Lee, C., Nancarrow, A. L., Ryan, D. P. and Sunde, M. (2008). Competition between LIM-binding domains. *Biochem. Soc. Trans.* **36**, 1393-1397.

Mizeracka, K., DeMaso, C. R. and Cepko, C. L. (2013). Notch1 is required in newly postmitotic cells to inhibit the rod photoreceptor fate. *Development* **140**, 3188-3197.

Monuki, E. S., Porter, F. D. and Walsh, C. A. (2001). Patterning of the dorsal telencephalon and cerebral cortex by a roof plate-Lhx2 pathway. *Neuron* **32**, 591-604.

Morrow, E. M., Furukawa, T., Lee, J. E. and Cepko, C. L. (1999). NeuroD regulates multiple functions in the developing neural retina in rodent. *Development* **126**, 23-36.

Muralidharan, B., Khatri, Z., Maheshwari, U., Gupta, R., Roy, B., Pradhan, S. J., Karmodiya, K., Padmanabhan, H., Shetty, A. S., Balaji, C. et al. (2017). LHX2 interacts with the NuRD complex and regulates cortical neuron subtype determinants Fezf2 and Sox11. *J. Neurosci.* **37**, 194-203.

Nagao, M., Ogata, T., Sawada, Y. and Gotoh, Y. (2016). Zbtb20 promotes astrocytogenesis during neocortical development. *Nat. Commun.* **7**, 11102.

Nelson, B. R., Hartman, B. H., Ray, C. A., Hayashi, T., Bermingham-McDonogh, O. and Reh, T. A. (2009). Acheate-scute like 1 (Ascl1) is required for normal delta-like (Dll) gene expression and notch signaling during retinal development. *Dev. Dyn.* **238**, 2163-2178.

Nelson, B. R., Ueki, Y., Reardon, S., Karl, M. O., Georgi, S., Hartman, B. H., Lamba, D. A. and Reh, T. A. (2011). Genome-wide analysis of Muller glial differentiation reveals a requirement for Notch signaling in postmitotic cells to maintain the glial fate. *PLoS ONE* **6**, e22817.

Ostendorff, H. P., Peirano, R. I., Peters, M. A., Schluter, A., Bossenz, M., Scheffner, M. and Bach, I. (2002). Ubiquitination-dependent cofactor exchange on LIM homeodomain transcription factors. *Nature* **416**, 99-103.

Porter, F. D., Drago, J., Xu, Y., Cheema, S. S., Wassif, C., Huang, S. P., Lee, E., Grinberg, A., Massalas, J. S., Bodine, D. et al. (1997). Lhx2, a LIM homeobox

gene, is required for eye, forebrain, and definitive erythrocyte development. *Development* **124**, 2935-2944.

Root, D. E., Hacohen, N., Hahn, W. C., Lander, E. S. and Sabatini, D. M. (2006). Genome-scale loss-of-function screening with a lentiviral RNAi library. *Nat. Methods* **3**, 715-719.

Roy, A., de Melo, J., Chaturvedi, D., Thein, T., Cabrera-Socorro, A., Houart, C., Meyer, G., Blackshaw, S. and Tole, S. (2013). LHX2 is necessary for the maintenance of optic identity and for the progression of optic morphogenesis. *J. Neurosci.* **33**, 6877-6884.

Subramanian, L., Sarkar, A., Shetty, A. S., Muralidharan, B., Padmanabhan, H., Piper, M., Monuki, E. S., Bach, I., Gronostajski, R. M., Richards, L. J. et al. (2011). Transcription factor Lhx2 is necessary and sufficient to suppress astrogliogenesis and promote neurogenesis in the developing hippocampus. *Proc. Natl. Acad. Sci. USA* **108**, E265-E274.

Thein, T., de Melo, J., Zibetti, C., Clark, B. S., Juarez, F. and Blackshaw, S. (2016). Control of lens development by Lhx2-regulated neuroretinal FGFs. *Development* **143**, 3994-4002.

Vasconcelos, F. F., Sessa, A., Laranjeira, C., Raposo, A. A. S. F., Teixeira, V., Hagey, D. W., Tomaz, D. M., Muhr, J., Broccoli, V. and Castro, D. S. (2016). MyT1 counteracts the neural progenitor program to promote vertebrate neurogenesis. *Cell Rep.* **17**, 469-483.

Ware, M., Hamdi-Roze, H., Le Friec, J., David, V. and Dupé, V. (2016). Regulation of downstream neuronal genes by proneural transcription factors during initial neurogenesis in the vertebrate brain. *Neural Dev.* **11**, 22.

Young, R. W. (1985). Cell proliferation during postnatal development of the retina in the mouse. *Brain Res.* **353**, 229-239.

Zuber, M. E., Gestri, G., Viczian, A. S., Barsacchi, G. and Harris, W. A. (2003). Specification of the vertebrate eye by a network of eye field transcription factors. *Development* **130**, 5155-5167.